Featured Article

Magnetic Resonance Imaging Measurements of the Response of Murine and Human Tumors to the Vascular-Targeting Agent ZD6126

Jeffrey L. Evelhoch,[1] Patricia M. LoRusso,[1] Zhanquan He,[1] Zachary DelProposto,[1] Lisa Polin,[1] Thomas H. Corbett,[1] Peter Langmuir,[2] Catherine Wheeler,[3] Andrew Stone,[4] Joanna Leadbetter,[4] Anderson J. Ryan,[4] David C. Blakey,[4] and John C. Waterton[4]

[1]Karmanos Cancer Institute, Wayne State University, Harper Hospital MR Center, Detroit, Michigan; [2]AstraZeneca, Wilmington, Delaware; [3]AstraZeneca Waltham, Massachusetts; and [4]Alderley Park, Macclesfield, Cheshire, United Kingdom

ABSTRACT

Purpose: **ZD6126 is a novel vascular targeting agent currently undergoing clinical evaluation. It acts by destabilizing the microtubulin of fragile and proliferating neoendothelial cells in tumors. The drug leads to blood vessel congestion, the selective destruction of the vasculature, and extensive necrosis in experimental tumors. The aim of the study reported here was to assess the ability of dynamic contrast enhanced magnetic resonance imaging (MRI) to measure the antivascular effects of ZD6126 in tumors.**

Experimental Design: **The work was carried out in mice bearing C38 colon adenocarcinoma and in patients with advanced cancers. MRI was performed before and 6 h (human tumors) or 24 h (C38 tumors) after i.v. drug administration. Contrast agent (gadolinium diethylenetriaminepentaacetate) enhancement was characterized by the initial area under the gadolinium diethylenetriaminepentaacetate uptake *versus* time curve (IAUC). IAUC reflects blood flow, vascular permeability, and the fraction of interstitial space.**

Results: **The median IAUC was reduced in all C38 tumors after ZD6126 administration [by 6–48% at 50 mg/kg ($n = 3$)], 58–91% at 100 mg/kg ($n = 4$), and 11–93% at 200 mg/kg ($n = 6$). In contrast, the administration of vehicle only led to no consistent change in median IAUC ($n = 4$). The ZD6126-induced changes in median IAUC appeared to be dose dependent ($P = 0.045$). No ZD6126-induced changes were apparent in murine muscle. Similar effects were seen in preliminary data from human tumors (11 tumors studied, 9 patients). At doses of 80 mg/m^2 and higher, the median IAUC post-ZD6126 treatment was reduced in all of the tumors studied (8 tumors, 6 patients) to 36–72% from the baseline value. There was a significant trend of increasing reductions with increasing exposure ($P < 0.01$). No drug-induced changes in human muscle or spleen IAUC were apparent. The reproducibility of the median IAUC parameter was investigated in patients. In 19 human tumors (measured in 19 patients) inter- and intratumor coefficients of variation were 64 and 18%.**

Conclusions: **The contrast enhanced-MRI measured median IAUC is a useful end point for quantifying ZD6126 antivascular effects in human tumors.**

INTRODUCTION

ZD6126 is a vascular targeting agent that was developed to disrupt the tubulin cytoskeleton of tumor neoendothelial cells. It is a phosphate prodrug of the potent tubulin-binding agent *N*-acetylcolchinol that inhibits tubulin polymerization and causes microtubule destabilization. Disrupting the fragile, proliferating neovasculature of malignant *versus* normal tissue confers tumor selectivity and distinguishes vascular targeting as a distinct cancer therapeutic approach from angiogenesis inhibition that is designed to prevent the formation of new blood vessels (1). *N*-Acetylcolchinol disrupts rapidly the tubulin cytoskeleton and morphology of human endothelial cells *in vitro* (2), and the morphological effects are selective for proliferating rather than confluent endothelial cells (3). Administration of ZD6126 *in vivo* causes rapid effects on tumor endothelium, leading to exposure of the basal lamina and loss of endothelial cells (4). The resulting thrombosis and vessel occlusion causes extensive tumor necrosis 24 h after ZD6126 administration. These effects are seen well below the maximum-tolerated dose and are selective for tumor blood vessels *in vivo* with no evidence of similar effects in normal tissue endothelium (4). The drug has antitumor activity against a broad range of human xenograft and rodent models (4), including lung cancer metastases (5). A consistent observation in preclinical models is a thin rim of peripheral tumor cells surviving treatment that subsequently leads to the regrowth of a tumor. The latter finding has stimulated combination studies of ZD6126 with antiproliferative cancer therapeutic approaches that are cytotoxic to the well-oxygenated, proliferating outer rim of experimental tumors. In support of the combined modality approach, the drug significantly improves the activity of cisplatin (4, 6), paclitaxel (7), and radiation (8) in tumor models. ZD6126 is currently under-

Received 10/16/03; revised 2/24/04; accepted 2/24/04.

Grant support: Supported by AstraZeneca (Alderley Park, Macclesfield, Cheshire, United Kingdom) and National Cancer Institute Grant UO1#CA62487-10.

The costs of publication of this article were defrayed in part by the payment of page charges. This article must therefore be hereby marked *advertisement* in accordance with 18 U.S.C. Section 1734 solely to indicate this fact.

Note: J. Evelhoch is currently at the World Wide Clinical Technology, Pfizer Global Research & Development, Ann Arbor, MI.

Requests for reprints: Patricia M. LoRusso, Karmanos Cancer Institute, Wayne State University, Harper Hospital MR Center, Detroit, MI 48201. Phone: (313) 745-1238; Fax: (313) 966-9317; E-mail: lorussop@karmanos.org.

going clinical evaluation, and preliminary studies of Phase I trials have been presented (1, 9, 10).

The clinical progress of antivascular therapy will be aided by the development and validation of methods for measuring changes in the vasculature of human tumors. Many methods are being investigated, in particular noninvasive imaging approaches such as magnetic resonance imaging (MRI), magnetic resonance angiography, magnetic resonance spectroscopy, Doppler ultrasound, and positron emission tomography (11). MRI is an attractive approach because it is widely available, it can provide whole-tumor, high-resolution pictures combining both spatial and functional information, and repeated measurements can be made (12). Although there are a number of MRI techniques that have potential in monitoring antivascular effects, contrast enhanced-MRI (DCE-MRI) is the most widely studied approach (13–15). Recommendations have now been developed for the appropriate MRI methodology for use in Phase I/II clinical trials assessing antiangiogenic and antivascular therapies (16). These recommendations state that one of two possible primary endpoints should be used which include the initial area under the contrast agent time curve (IAUC). IAUC reflects blood flow, vascular permeability, and the fraction of interstitial space.

The following study was established to assess the ability of MRI to measure the response of murine and human tumors to the vascular-targeting agent ZD6126. The hypotheses behind the studies were that the parameter IAUC could measure ZD6126 antivascular effects in tumors in a dose-dependent and reproducible fashion and that the results obtained in murine tumors could be translated into the clinic.

MATERIALS AND METHODS

Experimental Tumor Model. Studies in animals were carried out after approval by the Animal Use Committee of Wayne State University. The data were obtained using the murine C38 colon adenocarcinoma grown as s.c. tumors in the flanks of female B6D2F1 mice. ZD6126 (*N*-acetylcolchinol-*O*-phosphate) was formulated in a solution containing 20% of 5% sodium carbonate and 80% PBS at pH ~7. For the DCE-MRI experiments, ZD6126 was given as an i.v. tail vein injection at the following dose levels: 0 mg/kg ($n = 4$); 50 mg/kg ($n = 3$); 100 mg/kg ($n = 4$); and 200 mg/kg ($n = 6$). Control animals were treated with vehicle alone. For DCE-MRI experiments, animals were anesthetized (1.5% v/v halothane in oxygen) and immobilized on a bed heated by circulating temperature-controlled water. DCE-MRI was carried out immediately before and 24 h after i.v. ZD6126 administration. A comparative efficacy study was carried out of ZD6126 in C57/BL6 mice bearing C38 colon tumors. ZD6126 (100 or 200 mg/kg) was administered on day 10, when the median tumor size was 0.30 cm^3 (range, 0.18–0.41 cm^3). Necrosis was assessed by light microscopy. Tumor-bearing mice (three/group) were treated with ZD6126 or saline, and tumors were excised 24 h later. Tumors were fixed, processed, and scored as described previously (4). Slides were scored, subjectively and blinded, by a pathologist using the following grading system: (*a*) grade 1, 0–10% necrosis; (*b*) grade 2, >10–20%; (*c*) grade 3, >20–30%; (*d*) grade 4, >30–40%; (*e*) grade 5, >40–50%; (*f*) grade 6, >50–60%; (*g*) grade 7, >60–70%; (*h*) grade 8, >70–80%; (*i*) grade 9, >80–90%; and (*j*) grade 10; >90–100%. The mean ± SD grade for each dose group was calculated.

Patients. Studies in human tumors were carried out after ethical approval from Wayne State University Investigation Review Board and all patients gave informed consent. Preliminary data were available from 9 patients (4 male, 5 female) with liver metastases of mixed primary solid tumor origin (6 colorectal, 2 renal, 1 ovarian) who received a single i.v. dose of 56 mg/m^2 ($n = 3$), 80 mg/m^2 ($n = 3$), or 112 mg/m^2 ($n = 3$) ZD6126. MRI was performed 24–72 h before and 6 h after drug administration. The reproducibility of the method was evaluated in 19 patients with advanced solid tumors located in the liver ($n = 8$), bone ($n = 5$), soft tissue ($n = 3$), or pelvis ($n = 3$). DCE-MRI scans were performed twice separated by 2–6 days with no intervening treatment.

DCE-MRI of Murine C38 Tumors. The median tumor volume was 0.20 cm^3 (range, 0.07–0.99 cm^3). Images were acquired using an actively decoupled 3-cm surface coil for reception (together with a 12-cm actively decoupled birdcage volume coil for homogeneous excitation) on a Bruker Avance magnetic resonance scanner with a 4.7-T horizontal magnet. DCE-MRI data were collected continuously from five contiguous 2-mm slices through the tumor (five slices acquired every 6 s), at least one of which went through the abdomen to provide a muscle reference tissue. A spoiled gradient echo sequence was used with TE (echo time) = 1.5 ms, TR (repetition time) = 46.9 ms, and a 128 × 128 matrix (5 cm field of view). Two data sets were obtained precontrast [T_1 estimation (17) and precontrast background], and continuous images were taken before, during, and after a 0.3 mmol/kg bolus i.v. injection of the contrast agent, Gd-DTPA.

DCE-MRI of Human Tumors. MRI was performed on a 1.5-T Siemens Visionplus scanner using body coil excitation and phased array reception. Images were acquired using a spoiled gradient echo sequence (16 8-mm slices zero-filled to 32 4-mm slices, TE = 1.8 ms, TR = 3.8 ms, 128 × 256 matrix acquired zero-filled to 256 × 256 matrix with a 40-cm field of view) giving an acquisition time of 7.9 s/image set. Two data sets were obtained precontrast [T_1 estimation (17) and precontrast background], and continuous images were taken before, during, and after a bolus i.v. injection of 0.1 mmol/kg Gd-DTPA.

DCE-MRI Data Analysis. For each tumor slice, a region of interest was drawn using T_1-estimated data and/or the final enhancement over the whole tumor, excluding the surrounding normal tissue. Tumor volumes were estimated by voxel counting. Similar regions of interest were drawn over back muscle (murine human) and spleen (human), where available within the imaged field of view. The preinjection images were averaged to increase the signal to noise ratio and subtracted from the postinjection images to give enhancement images. Tumor and muscle contrast agent enhancement time courses were calculated voxelwise using the enhancement and baseline T_1 values. The change in signal (SGd-S0) was divided by the original signal (S0) so that the inhomogeneous sensitivity of the surface coil was divided out. The data were converted to contrast agent concentrations using the known relaxivity of Gd-DTPA: (SGd-S)/S0 was converted to $\Delta R1$ using a look-up table for the observed

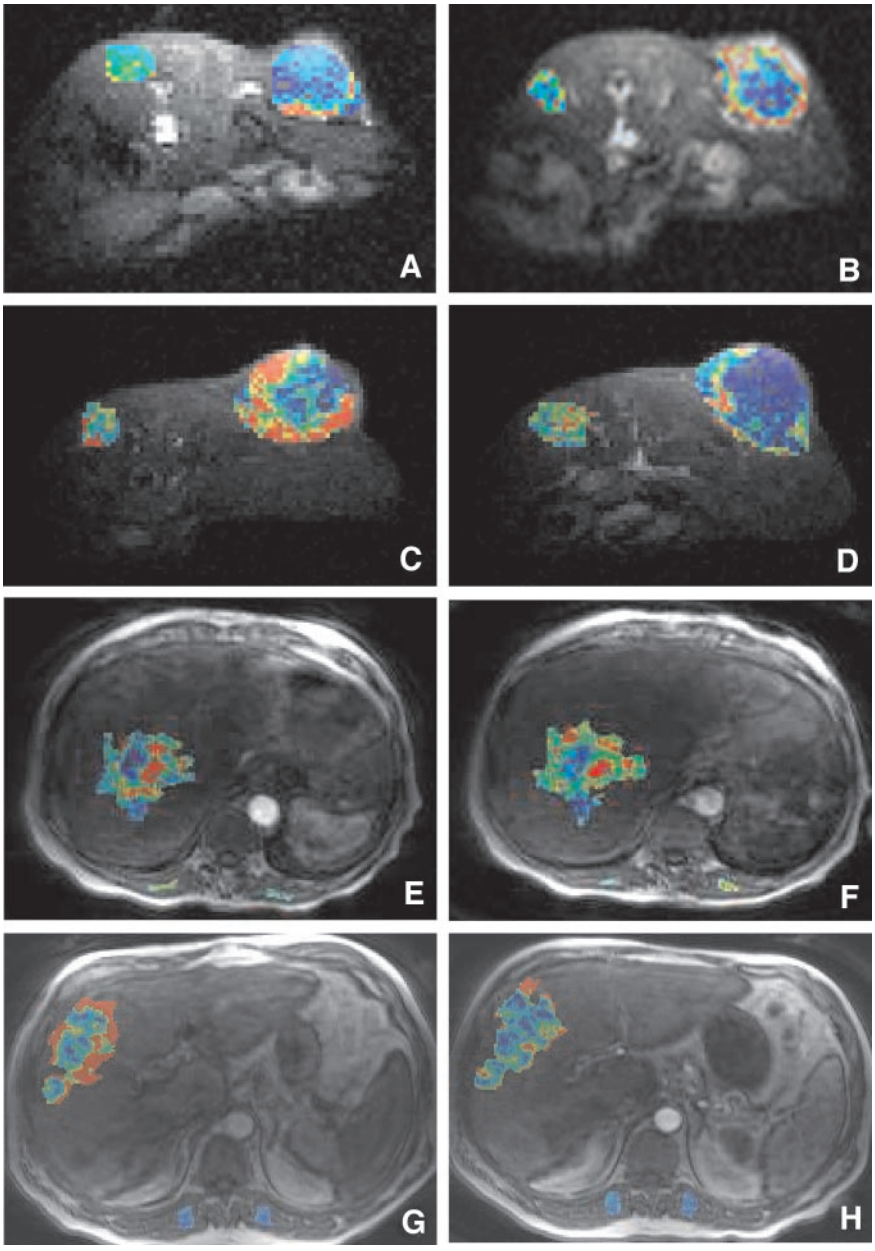

Fig. 1 Representative images from single slices through the following: a C38 tumor pre- and posttreatment with 0 mg/kg ZD6126 (*A* and *B*); a C38 tumor pre- and posttreatment with 200 mg/kg ZD6126 (*C* and *D*), a human liver metastasis (patient 17) scanned twice 2 days apart with no intervening treatment (*E* and *F*); and a human liver metastasis (patient 1) pre- and posttreatment with 56 mg/m^2 ZD6126 (*G* and *H*). The IAUC color scale increases from green to yellow to red.

initial R1, and ΔR1 was converted to contrast agent (CA) using the relationship published by Donahue *et al.* (18). The IAUC (*i.e.*, first 60 s after bolus arrival) of tissue contrast was calculated on a voxel-wise basis, and the median values were obtained. The effect of increasing dose on changes in enhancement was investigated by fitting a statistical model to the log of the ratio of posttreatment to pretreatment median IAUC values with a linear term for dose. In the reproducibility study, the coefficient(s) of variation (CV) was calculated as the appropriate SD divided by the mean and expressed as a percentage. Any between tumor CV were calculated using the first scan of each tumor. There were 2 patients who had multiple tumors assessed, and for these patients, the average of the median tumor IAUC was used.

RESULTS

A single dose of ZD6126 (100 or 200 mg/kg) induced extensive tumor necrosis within 24 h in mice bearing C38 tumors. Histological examination revealed a core of central necrosis surrounded by a viable rim of tumor 24 h after ZD6126 administration. The mean ± SD tumor necrosis scores were 3.7 ± 2.1, 7.0 ± 2.6, and 9.7 ± 0.6 after 0, 100, and 200 mg/kg ZD6126, respectively. The level of necrosis after 200 mg/kg ZD6126 was significantly higher than in controls ($P = 0.009$, t

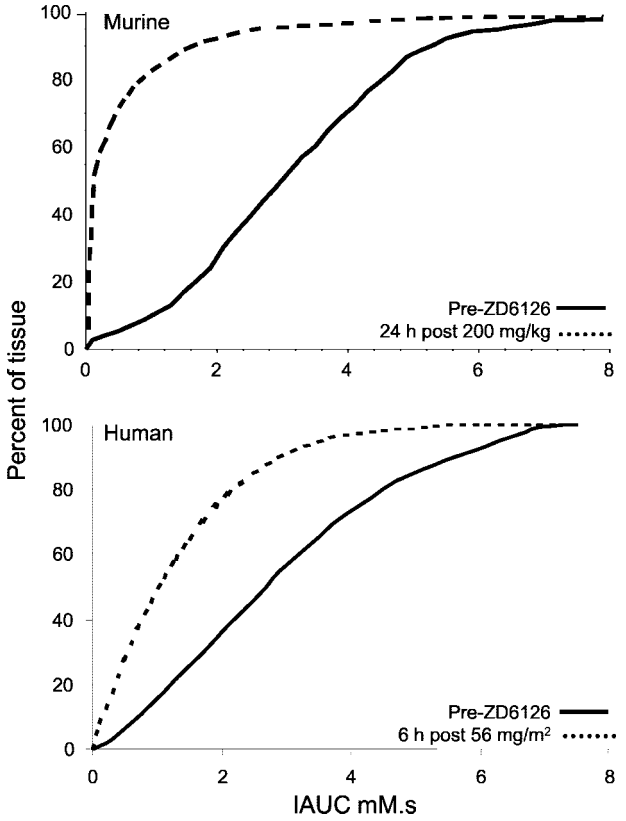

Fig. 2 Cumulative frequency curves (*i.e.*, a plot of the total number of values that are at or below a given value) of initial area under the contrast agent time curve (IAUC) values for a murine C38 tumor scanned pre- and 24 h postadministration of 200 mg/kg ZD6126 (*top*). The median initial area under the contrast agent time curve (IAUC) values pre- and posttreatment were 3.08 and 0.21 mM. Cumulative frequency of IAUC values for a human liver metastasis (patient 1) scanned pre- and 6 h postadministration of 56 mg/m^2 ZD6126 (*bottom*). The median IAUC values pre- and posttreatment were 2.78 and 1.13 mM. See Fig. 1 for the images from these tumors.

test). Despite the ZD6126-induced tumor cell necrosis, there was no inhibition of tumor growth with growth delays of 0 and 1 day after the single 100 and 200 mg/kg treatments, respectively.

DCE-MRI was performed before and 24 h after ZD6126 administration. The images showed contrast agent uptake in tumors and ZD6126 elimination of contrast uptake in the center of the murine tumors with only a high enhancing rim remaining 24 h after treatment (Fig. 1). Time courses for the changes in contrast agent concentration with time were obtained from the pre- and posttreatment images as described in the "Materials and Methods," and values for IAUC calculated on a voxel-wise basis. Fig. 2 illustrates typical C38 tumor IAUC cumulative frequency curves pre- and postadministration of ZD6126. The substantial left shifting of the curve 24 h after treatment shows a drug-induced reduction in contrast agent uptake, consistent with a reduction in tumor perfusion. Median IAUC was calculated for each tumor before and 24 h after treatment, and the data are summarized in Table 1. Twenty-four h after ZD6126 administration, there was a reduction in median IAUC in all of the C38 tumors studied (Table 1, Fig. 3) by 6–48% at 50 mg/kg, 58–91% at 100 mg/kg, and 11–93% at 200 mg/kg. After administration of the vehicle alone, there was no consistent change in median IAUC. There was a significant trend of increasing reductions with increasing dose ($P = 0.045$). There were no apparent changes in muscle IAUC (Table 1, Fig. 3) or in MRI measurements of tumor volume made pre- and post-ZD6126 administration.

Similar findings were seen in the human tumors. Six h after ZD6126 administration, there was a reduction in contrast enhancement in the magnetic resonance images (Fig. 1) and a left shifting of the IAUC cumulative frequency curve (Fig. 2). The preliminary human ZD1626 data are listed in Tables 2 and 3. Tumor IAUC 6 h after ZD6126 administration was lower then pretreatment IAUC in all of the tumors. The ZD6126-induced reduction in tumor IAUC ranged from 1 to 72%. ZD6126-induced changes in IAUC appeared to increase with increasing dose (Fig. 3). This trend was tested using the data from the 19 tumors in the reproducibility study as zero dose data (Table 3), and the trend was significant ($P < 0.01$). No ZD6126-induced changes were apparent in muscle IAUC. Similarly, there was no consistent change in splenic IAUC after ZD6126 administration (Table 2, Fig. 3)

The reproducibility of the method was examined in 19 patients (one tumor/patient) with advanced cancers scanned on two separate occasions 2–6 days apart with no intervening treatment (Table 3). Values for IAUC were more variable between than within tumors with CV of 64 and 18%, respectively. The corresponding figures for human muscle were 39 and 14%.

DISCUSSION

Determining the clinical activity of vascular-targeting agents will be aided by the development and validation of

Table 1 Murine ZD6126 study data[a]

Dose (mg/kg)	Tumor IAUC (mM)			Muscle IAUC (mM)		
	Pre	Post	Change	Pre	Post	Change
0	0.89	1.56	+74%	0.80	0.92	+15%
0	1.56	2.42	+55%	1.15	1.05	−9%
0	1.78	3.85	+116%	0.75	1.31	+75%
0	2.53	1.66	−34%	0.93	0.61	−34%
50	1.27	1.19	−6%	1.18	1.26	+6%
50	1.35	0.70	−48%	1.04	0.62	−41%
50	1.89	1.25	−34%	0.95	1.01	+6%
100	0.94	0.39	−58%	1.50	1.59	+6%
100	2.45	0.34	−86%	1.96	2.30	+18%
100	2.15	0.18	−91%	1.12	1.29	+16%
100	1.63	0.24	−85%	1.34	1.52	+13%
200	0.79	0.56	−29%	0.89	0.93	+4%
200	0.98	0.87	−11%	0.60	1.10	+83%
200	1.80	0.46	−75%	0.79	0.80	+1%
200	3.08	0.21	−93%	1.41	0.95	−32%
200	2.81	0.85	−70%	1.01	1.01	0%
200	2.96	1.87	−37%	0.97	1.73	+79%

[a] Contrast enhanced-magnetic resonance imaging measurements of median initial area under the contrast agent time curve (IAUC) were made before (pre) and 24 h after (post) ZD6126 administration to C38-bearing animals.

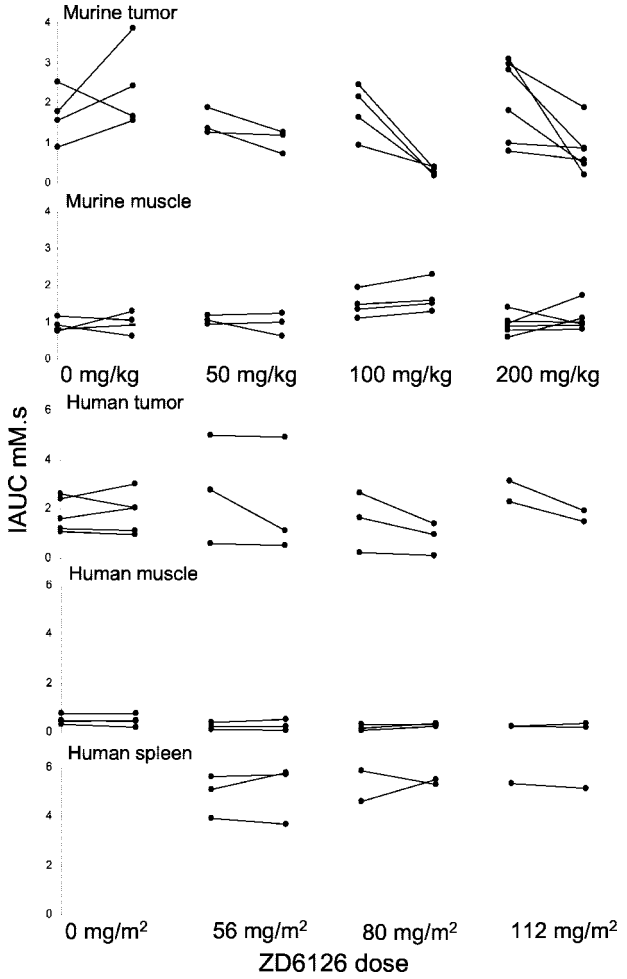

Fig. 3 The change in initial area under the contrast agent time curve (IAUC) as a function of ZD6126 dose in murine C38 tumor and muscle and human tumor, muscle, and spleen. IAUC was measured before and 24 h (murine) or 6 h (human) after treatment with ZD6126. For clarity of presentation, a subset of the human reproducibility data listed in Table 3 is shown for the 0 dose point. The control data were obtained from repeat scans of colorectal cancer liver metastases made 2–5 days apart with no intervening treatment.

clinically applicable MRI parameters that measure relevant tumor vasculature-related end points. This development is important because vascular-targeting agents lack the antiproliferative cytotoxicity associated with conventional anticancer approaches. Antivascular effects are seen at doses well below the maximum-tolerated dose in animals (4, 19, 20), and the adverse events used in clinical dose-finding studies of cytotoxic approaches are less likely to be applicable. The results reported here show the potential of using DCE-MRI in ZD6126 dose-finding studies in humans. Although a number of studies have already shown the potential of using DCE-MRI with the vascular-targeting agents CA4P (7, 13–15, 21–23) and DMXAA (22, 24), there is only one published study for ZD6126 (25). In addition, we have shown that ZD6126 dose-dependent changes can be measured using MRI and that the approach developed in murine tumors can be translated into the clinic. The results reported here, therefore, support the use of DCE-MRI as a pharmacodynamic tool in humans.

In the murine tumors studied the ZD6126 dose-dependent changes were measured in the absence of any therapeutic activity. ZD6126 administration to tumor-bearing animals resulted in the expected rapid induction of a central core of tumor necrosis surrounded by a rim of viable tumor. The latter observation is consistent with published results reported for ZD6126 (4, 7, 26) and other vascular-targeting agents (1). The single ZD6126 dose administration, however, did not lead to any subsequent inhibition of tumor growth. Again, this is consistent with an expected rapid tumor repopulation from the surviving viable rim (4, 7, 26). It is expected not only that repeat administration will be important for the clinical efficacy of ZD6126 but also that the greatest therapeutic benefit will come from the development of combination treatments involving the coadministration of antiproliferative treatments such as radiation (1, 8), paclitaxel (7), or cisplatin (4, 6).

The dose-dependent changes measured in the murine and human tumors are consistent with the results of a study of ZD6126 in a rat prolactinoma model (25) and the preliminary findings from a Phase I trial for CA4P (23). In contrast, there was no evidence of a dose response reduction in tumor IAUC after the administration of DMXAA to patients (24). These differences might relate to the mechanisms of action of the drugs. Both CA4P and ZD6126 are microtubule-destabilizing agents, whereas DMXAA acts by stimulating tumor and host cells to synthesize tumor necrosis factor. Tumor necrosis factor promotes the production of procoagulant factors and disrupts cytoskeletal connections, leading to increased vascular permeability.

This study used the parameter IAUC that measures Gd-DTPA inflow and also the bulk perfusion of a tumor (14). Although to date less widely used than modeled kinetic parameters, it is being used increasingly when measuring the antitumor effects of vascular-targeting agents (14, 15, 22, 24, 27). The most widely used modeled kinetic parameter is the transfer constant K^{trans} that reflects Gd-DTPA delivery (perfusion), transport across the vascular endothelium (vascular permeability), and blood volume (28–30). IAUC reflects the same parameters as K^{trans} and also the fraction of interstitial space. Either IAUC or K^{trans} has been recommended as the primary end point for use in Phase I/II clinical trials of antivascular agents (16). The measurement of ZD6126-induced reductions in IAUC in murine and human tumors validates its use in Phase I/II clinical trials.

The IAUC parameter was reproducible in patients. The within tumor CV for IAUC were 18%, which is similar to the value of 12% for IAUC and 24% for K^{trans} for repeat measurements in 16 human tumors reported elsewhere (27). It is also of note that in the Galbraith *et al.* (27) study a comparison was made of voxel-wise (as used here) and whole tumor analysis. The authors recommended that a voxel-wise rather than a whole tumor approach is used because it is both more reproducible and also enables the evaluation of tumor heterogeneity in parametric images (27). A within tumor CV of 17% was reported in rat GH3 prolactinomas (25), suggesting that the reproducibility of the method is similar in human and animal tumors. The between tumor CV in the human tumors studied here was higher (CV = 64%) than in animals tumors studied here (CV = 41%) or elsewhere (CV = 26%; Ref. 25). The greater between tumor

Table 2 Human ZD6126 study data[a]

Patient no.	Gender	Tumor[b]	Tumor type	Tumor size[c] Pre	Tumor size[c] Post	Dose (mg/m^2)	Tumor IAUC (mM) Pre	Tumor IAUC (mM) Post	Tumor IAUC (mM) Change	Muscle IAUC (mM) Pre	Muscle IAUC (mM) Post	Muscle IAUC (mM) Change	Spleen IAUC (mM) Pre	Spleen IAUC (mM) Post	Spleen IAUC (mM) Change
1	M	M	Colon carcinoma	149.1	133.5	56	2.78	1.13	−59%	0.25	0.26	+5%	5.10	5.79	+14%
2	M	M	Renal cell carcinoma	161.6	148.5	56	4.98	4.92	−1%	0.41	0.53	+28%	3.95	3.70	−6%
3	F	M	Colon carcinoma	7.4	7.9	56	0.59	0.54	−9%	0.11	0.08	−29%	5.64	5.72	+1%
4	M	M	Colon carcinoma	4.5	5.6	80	1.62	1.04	−36%	0.15	0.37	+144%	4.64	5.52	+19%
4		M		3.1	3.8	80	1.74	0.92	−47%						
5	F	M	Ovarian carcinoma	23.8	23.3	80	0.26	0.13	−51%	0.09	0.26	+192%			
6	F	M	Colon carcinoma	20.4	20.5	80	1.60	0.44	−72%	0.31	0.34	+7%	5.88	5.30	−10%
6		M		253.9	262.8	80	3.74	2.38	−37%						
7	F	M	Rectal carcinoma	1.7	2.1	112	2.30	1.48	−36%	0.22	0.35	+59%	5.35	5.14	−4%
8	M	M	Colon carcinoma	5.5		112	4.48			0.63					
9	F	M	Renal cell carcinoma	80.8	80.3	112	3.15	1.92	−39%	0.24	0.20	−16%			

[a] Contrast enhanced-magnetic resonance imaging measurements of median initial area under the contrast agent time curve (IAUC) were made before (pre) and 6 h after (post) ZD6126 administration to patients with advanced cancers. In some cases, data were not obtained because of magnetic resonance imaging unavailability or the tissue was not in the imaged field of view.
[b] Imaged tumor whether primary (P) or metastatic (M).
[c] Tumor size in cm^3.

variability in human *versus* animal tumors is as expected when comparing inhomogeneous human tumors with transplantable animal tumors.

In comparison with IAUC, modeled DCE-MRI kinetic parameters such as K^{trans} require an arterial input function (AIF). The AIF minimizes variations between patients because of variable systemic blood supplies and the delivery of the contrast agent to a tumor. AIFs can be obtained by drawing regions of interest over major arterial blood vessels such as the carotid and vertebral arteries for head and neck imaging or the external iliac artery for imaging in the abdomen. As it is often difficult to measure an AIF in patients, a general function is used. However, it has been shown that normalizing DCE-MRI data using an individual rather than a general AIF improves substantially the reproducibility of the measurement of vascular parameters (31). Although the IAUC parameter does not require an AIF, an AIF might be useful for the normalization of the data obtained in repeat scans of the same patient. In theory, allowing for differences in the systemic delivery of the contrast agent between scans should additionally improve on the reproducibility and pharmacodynamic use of IAUC. We have previously shown in murine tumors that the IAUC parameter, when normalized to muscle tissue to account for differences in AIF between studies, parallels estimates of K^{trans} over a wide range of tissue input functions (32). Although the normalization of IAUC to muscle tissue was effective in murine models, how-

Table 3 Human reproducibility data[a]

Patient no.	Gender	Tumor	Tumor type	Imaged site	Days[b]	Tumor size[c] First	Tumor size[c] Second	Tumor IAUC[d] First	Tumor IAUC[d] Second	Muscle IAUC[d] First	Muscle IAUC[d] Second
10	F	M	Bronchoalveolar	Liver	3	36	36	5.42	3.13	0.92	0.76
11	M	M	Colon carcinoma	Liver	4	41	40	2.63	2.04	0.31	0.21
12	M	P	Alveolar sarcoma	Soft tissue	3	321	332	4.36	3.97	0.87	0.78
13	F	M	Colon carcinoma	Liver	2	35	37	1.08	0.96	0.50	0.44
14	M	P	Renal cell carcinoma	Liver	3	17	18	8.20	8.27	0.41	0.34
15	M	P	Renal cell carcinoma	Soft tissue	2	190	199	9.00	8.34	0.66	0.50
16	F	M	Colon carcinoma	Pelvic	2	17	17	3.05	2.67	0.63	0.65
17	F	M	Colon carcinoma	Liver	2	150	143	1.19	1.12	0.77	0.79
18	M	M	Renal cell carcinoma	Bone	2	6	6	5.43	3.70	1.15	1.10
19	F	M	Colon carcinoma	Pelvic	2	20	19	3.34	2.84	1.21	1.27
20	F	M	Ovarian carcinoma	Liver	2	66	68	5.96	4.93	1.18	0.86
21	F	M	Breast carcinoma	Bone	2	13	13	3.27	4.47	0.69	0.70
22	M	M	Colon carcinoma	Liver	4	345	386	1.60	2.07	0.44	0.48
23	M	M	Colon carcinoma	Liver	5	36	37	2.41	3.01	0.45	0.47
24	M	M	Melanoma	Soft tissue	2	230	207	5.20	4.12	0.90	0.74
25	F	M	Breast carcinoma	Bone	2	22	21	2.14	1.91	1.22	1.29
26	M	M	Lung carcinoma	Bone	6	3	3	1.93	1.30	0.84	0.55
27	M	M	Colon carcinoma	Pelvic	3	162	173	1.02	0.92	0.73	0.59
28	M	M	Prostate carcinoma	Bone	3	11	11	2.55	2.63	0.47	0.36

[a] Imaged tumor whether primary (P) or metastatic (M).
[b] Number of days between repeat scans.
[c] Tumor size in cm^3.
[d] Median initial area under the contrast agent time curve (IAUC) in mM.

ever, it was not used here because the low perfusion of human (Table 2) in comparison with murine (Table 1) muscle was associated with an increase in noise and variability. This is illustrated by the range of values for the percent change in IAUC between repeat scans of −41 to +83% for murine muscle (n = 17) *versus* −29 to +192% for human muscle (n = 8). A method has been described for the derivation of an AIF from tissue using a simple algorithm for its automatic extraction from DCE-MRI data (31). In view of the high perfusion and reproducibility of repeat scan data in human spleen (Table 2), it would of interest in the future to examine whether an AIF derived from healthy spleen tissue would be of value.

Additional improvement of the pharmacodynamic use of IAUC measurements in tumors might also be expected from using ZD6126 pharmacokinetic (*i.e.*, drug exposure) rather than dose data. Although the complete pharmacokinetic data are not yet available for all of the patients studied here, the plasma levels of the active metabolite of ZD6126 were available for some. It is of interest to note that of the patients receiving 56 mg/m^2 ZD6126, patient 1 who showed a good tumor response to ZD6126 (Table 2) had plasma levels of the ZD6126 metabolite that were nearly double those of patients 2 and 3.

In conclusion the DCE-MRI measurement of IAUC is a robust and simple technique for use in humans. The approach developed in murine models has been easily translated into clinical use. IAUC can measure ZD6126 dose-dependent effects in human tumors in a reproducible manner. Therefore, a useful end point for quantifying the biological activity of ZD6126 in Phase I/II clinical trials is the measurement of IAUC using DCE-MRI.

ACKNOWLEDGMENTS

We thank Cristina Filetti for her assistance in producing the magnetic resonance images and Russell Westwood for performing the tumor histology and necrosis measurements.

REFERENCES

1. Thorpe PE, Chaplin DJ, Blakey DC. The first international conference on vascular targeting: meeting overview. Cancer Res 2003;63: 1144–7.

2. Micheletti G, Poli M, Borsotti P, et al. Vascular-targeting activity of ZD6126, a novel tubulin-binding agent. Cancer Res 2003;63:1534–7.

3. Blakey DC, Douglas S, Revill M, Ashton SE. The novel vascular targeting agent ZD6126 causes rapid morphology changes leading to endothelial cell detachment at non-cytotoxic concentrations [abstract]. Clin Exp Metastasis 2000;17:776.

4. Blakey DC, Westwood FR, Walker M, et al. Antitumor activity of the novel vascular targeting agent ZD6126 in a panel of tumor models. Clin Cancer Res 2002;8:1974–83.

5. Goto H, Yano S, Zhang H, et al. Activity of a new vascular targeting agent, ZD6126, in pulmonary metastases by human lung adenocarcinoma in nude mice. Cancer Res 2002;62:3711–5.

6. Siemann DW, Rojiani AM. Antitumor efficacy of conventional anticancer drugs is enhanced by the vascular targeting agent ZD6126. Int J Radiat Oncol Biol Phys 2002;54:1512–7.

7. Davis PD, Dougherty GJ, Blakey DC, et al. ZD6126: a novel vascular-targeting agent that causes selective destruction of tumor vasculature. Cancer Res 2002;62:7247–53.

8. Siemann DW, Rojiani AM. Enhancement of radiation therapy by the novel vascular targeting agent ZD6126. Int J Radiat Oncol Biol Phys 2002;53:164–71.

9. Radema SA, Beerepoot LV, Witteveen PO, Gebbink MF, Wheeler C, Voest EE. Clinical evaluation of the novel vascular-targeting agent, ZD6126: assessment of toxicity and surrogate markers of vascular damage. Proc Am Soc Clin Oncol 2002;21:110a.

10. Gadgeel SM, LoRusso PM, Wozniak AJ, Wheeler C. A dose-escalation study of the novel vascular-targeting agent, ZD6126, in patients with solid tumors. Proc Am Soc Clin Oncol 2002;21:110a.

11. Anderson H, Price P, Blomley M, Leach MO, Workman P. Measuring changes in human tumour vasculature in response to therapy using functional imaging techniques. Br J Cancer 2001;85:1085–93.

12. Padhani AR. Dynamic contrast-enhanced MRI in clinical oncology: current status and future directions. J Magn Reson Imaging 2002;16: 407–22.

13. Maxwell RJ, Wilson J, Prise VE, et al. Evaluation of the antivascular effects of combretastatin in rodent tumours by dynamic contrast enhanced MRI. NMR Biomed 2002;15:89–98.

14. Beauregard DA, Thelwall PE, Chaplin DJ, Hill SA, Adams GE, Brindle KM. Magnetic resonance imaging and spectroscopy of combretastatin A4 prodrug-induced disruption of tumour perfusion and energetic status. Br J Cancer 1998;77:1761–7.

15. Beauregard DA, Hill SA, Chaplin DJ, Brindle KM. The susceptibility of tumors to the antivascular drug combretastatin A4 phosphate correlates with vascular permeability. Cancer Res 2001;61: 6811–5.

16. Leach MO, Brindle KM, Evelhoch JL, et al. Assessment of antiangiogenic and anti-vascular therapeutics using magnetic resonance imaging: recommendations for appropriate methodology for clinical trials. Proc Am Assoc Cancer Res 2003;44:115.

17. Brookes JA, Redpath TW, Gilbert FJ, Murray AD, Staff RT. Accuracy of T1 measurement in dynamic contrast-enhanced breast MRI using two- and three-dimensional variable flip angle fast low-angle shot. J Magn Reson Imaging 1999;9:163–71.

18. Donahue KM, Weisskoff RM, Burstein D. Water diffusion and exchange as they influence contrast enhancement. J Magn Reson Imaging 1997;7:102–10.

19. Chaplin DJ, Pettit GR, Hill SA. Anti-vascular approaches to solid tumour therapy: evaluation of combretastatin A4 phosphate. Anticancer Res 1999;19:189–95.

20. Dark GG, Hill SA, Prise VE, Tozer GM, Pettit GR, Chaplin DJ. Combretastatin A-4, an agent that displays potent and selective toxicity toward tumor vasculature. Cancer Res 1997;57:1829–34.

21. Galbraith SM, Maxwell RJ, Lodge MA, et al. Combretastatin A4 phosphate has tumor antivascular activity in rat and man as demonstrated by dynamic magnetic resonance imaging. J Clin Oncol 2003;21: 2831–42.

22. Beauregard DA, Pedley RB, Hill SA, Brindle KM. Differential sensitivity of two adenocarcinoma xenografts to the anti-vascular drugs combretastatin A4 phosphate and 5,6-dimethylxanthenone-4-acetic acid, assessed using MRI and MRS. NMR Biomed 2002;15: 99–105.

23. Dowlati A, Robertson K, Cooney M, et al. A Phase I pharmacokinetic and translational study of the novel vascular targeting agent combretastatin a-4 phosphate on a single-dose intravenous schedule in patients with advanced cancer. Cancer Res 2002;62:3408–16.

24. Galbraith SM, Rustin GJ, Lodge MA, et al. Effects of 5,6-dimethylxanthenone-4-acetic acid on human tumor microcirculation assessed by dynamic contrast-enhanced magnetic resonance imaging. J Clin Oncol 2002;20:3826–40.

25. Robinson SP, McIntyre DJ, Checkley D, et al. Tumour dose response to the antivascular agent ZD6126 assessed by magnetic resonance imaging. Br J Cancer 2003;88:1592–7.

26. Blakey DC, Ashton SE, Westwood FR, Walker M, Ryan AJ. ZD6126: a novel small molecule vascular targeting agent. Int J Radiat Oncol Biol Phys 2002;54:1497–502.

27. Galbraith SM, Lodge MA, Taylor NJ, et al. Reproducibility of dynamic contrast-enhanced MRI in human muscle and tumours: com-

parison of quantitative and semi-quantitative analysis. NMR Biomed 2002;15:132–42.

28. Knopp MV, Giesel FL, Marcos H, von Tengg-Kobligk H, Choyke P. Dynamic contrast-enhanced magnetic resonance imaging in oncology. Top Magn Reson Imaging 2001;12:301–8.

29. Gossmann A, Helbich TH, Kuriyama N, et al. Dynamic contrast-enhanced magnetic resonance imaging as a surrogate marker of tumor response to anti-angiogenic therapy in a xenograft model of glioblastoma multiforme. J Magn Reson Imaging 2002;15:233–40.

30. Drevs J, Muller-Driver R, Wittig C, et al. PTK787/ZK 222584, a specific vascular endothelial growth factor-receptor tyrosine kinase inhibitor, affects the anatomy of the tumor vascular bed and the functional vascular properties as detected by dynamic enhanced magnetic resonance imaging. Cancer Res 2002;62:4015–22.

31. Rijpkema M, Kaanders JH, Joosten FB, van der Kogel AJ, Heerschap A. Method for quantitative mapping of dynamic MRI contrast agent uptake in human tumors. J Magn Reson Imaging 2001;14:457–63.

32. Evelhoch JL, He Z, Polin L, Corbett TH, Blakey DC, Waterton JC. Dynamic contrast-enhanced MRI evaluation of the effects of ZD6126 on tumor vasculature. Proc Int Soc Magn Reson Med 2001;9:481.